Etude multi-échelles de l'influence de la décohésion interfaciale sur la piézorésistivité de nanocomposites polymère/graphène

Xiaoxin Lu, Fabrice Detrez, Julien Yvonnet, Jinbo Bai

Etude multi-échelles de l'influence de la décohésion interfaciale sur la piézorésistivité de nanocomposites polymère/graphène

Xiaoxin LU[a,b], Fabrice DETREZ[b,⋆], Julien YVONNET[b], Jinbo BAI[a]

a. Université Paris Saclay, Laboratoire de Mécanique des Sols, Structures et Matériaux, UMR 8579 CNRS, 8-10 rue Joliot Curie, 91190 Gif-sur-Yvette, France
b. Université Paris-Est, Laboratoire de Modélisation et Simulation Multi Echelle, UMR 8208 CNRS, 5 Boulevard Descartes, 77454 Marne-la-Vallée Cedex 2, France
⋆ fabrice.detrez@u-pem.fr

Résumé :

Une stratégie multi-échelles est proposée pour étudier le rôle de la décohésion interfaciale sur les propriétés piézorésistives du nanocomposite graphène/polymère. L'effet piézorésistif est la modification de la résistivité électrique lorsque des contraintes mécaniques sont appliquées. Premièrement, un modèle de zone cohésive est identifié à l'aide de simulations atomistiques. Ce modèle de zone cohésive sert à enrichir le modèle d'interfaces imparfaites, modélisant les graphènes, à l'échelle mésoscopique de notre modèle de mécanique. Ce modèle non linéaire est utilisé pour générer des Volumes Elémentaires Représentatifs déformés afin d'étudier l'influence de la déformation et de la décohésion interfaciale sur la conductivité des nanocomposites polymère/graphène. La conductivité effective est étudiée avec un modèle électrique continue à l'échelle mésoscopique incorporant l'effet tunnel. Une transition conducteur-isolant est observée pour des allongements supérieurs à 2% pour la fraction volumique de graphène juste au-dessus du seuil de percolation. La transition apparaît pour un allongement de 8% au lieu de 2%, lorsque la décohésion interfaciale est négligée.

Abstract :

A multiscale strategy is proposed to study the role of interfacial decohesion on the piezoresistive properties of graphene/polymer nanocomposite. A cohesive zone model is identified by atomistic simulations. This cohesive zone model enriches imperfect interfaces, which model graphene sheets, at mesoscale in our continuum mechanical model. This nonlinear mechanical model is used to generate deformed representative volume element to study influence of strain and interfacial decohesion on the conductivity of graphene/polymer nanocomposites. The effective conductivity is studied with an electric continuum model at mesoscale that incorporates the tunneling effect. A conductor-insulator transition is observed for elongations above 2% for graphene volume fraction just above the percolation threshold. The transition appears for an elongation of 8% instead of 2%, when the interfacial decohesion is removed.

Mots clefs : Polymère/graphène nanocomposites, Interfaces imparfaites, Modèle de zone cohesive, Couplage electro-mécanique

1 Introduction

Graphene/polymer nanocomposites have recently attracted a growing attention due to their high electric conductivity for very low volume fraction and their interesting mechanical performances. A wide range of smart materials have been developed for practical applications with the introduction of graphene or other carbon allotropes. In particular, the research on strain sensing behavior of graphene/polymer nanocomposites has been carried out based on monitoring the strain-induced resistivity change, *i.e.* piezoresistive effect, showing potential in the area of structural health monitoring.

Although many experiments have been conducted to study these new materials, the mechanisms underlying the piezoresistive effect are still not well understood. Their influences on effective properties remain an open domain. This study proposes a multiscale and mutli-physical strategy, in order to understand the role of interfacial decohesion on the piezoresistive properties of graphene/polymer nanocomposite [1]. The main issues of this aim are :

- the identification of the mechanical behavior laws associated with the nanometric decohesion mechanism between graphene and the polymer ;
- the numerical simulation of Representative Volume Element (RVE) containing very thin objects such as graphene sheets ;
- the modeling of quantum effects, such as the tunneling effect, at the continuum mesoscale.

In that context, a multiscale and multiphysics simulation framework, from nanoscale up to the macroscale, can help us to tackle these issues. The contribution and the originality of this work is to combine and to transpose three modeling framework :

- the identification by Molecular Dynamics (MD) of a Cohesice Zone (CZ) model between graphene and polymer ;
- the imperfect interfaces to model the graphene sheets like a 2D object to avoid to finer mesh for the resolution of the mesoscopic problem by Finite Element Method (FEM) [2, 3, 4] ;
- the introduction, at the continuum mesoscoale, of the tunneling effect to model of electrical conductivity through a distance function, $d(x)$ [2, 3, 4].

Figure 1 presents a scheme of our bottom-up approach, which is able to predicts the variation of electrical conductivity and percolation threshold of the polymer/graphene nanocomposites under applied strain. The effective electrical conductivity is computed by nonlinear FEM framework, which takes into account the tunneling effect [2, 3, 4, 5], at mesoscale on the deformed RVEs. The tunneling effect, which is quantum phenomena, is created through very thin isolating barriers like polymer layers when the distance between the two conducting phases lower than several nanometers. It leads to unexpected values of electrical conductivity for very small volume fractions of graphene.

2 Identification of a nonlinear cohesive model by molecular dynamic

In the present section, a nonlinear CZ model for the interface between graphene and polymer is identified by MD simulations. For this purpose, we study a sample where a graphene sheet is placed on the top of PE slab (see Fig. 2 (a)). A coarse-grained model is used for PE macromolecules, which are represented by 500 beads of $-\mathrm{CH_2}-$ atom units. The system contains 80 PE chains and 4860 carbon atoms in the graphene sheet. The system is periodical on X-Y plane and non-periodical on Z direction. Dreiding

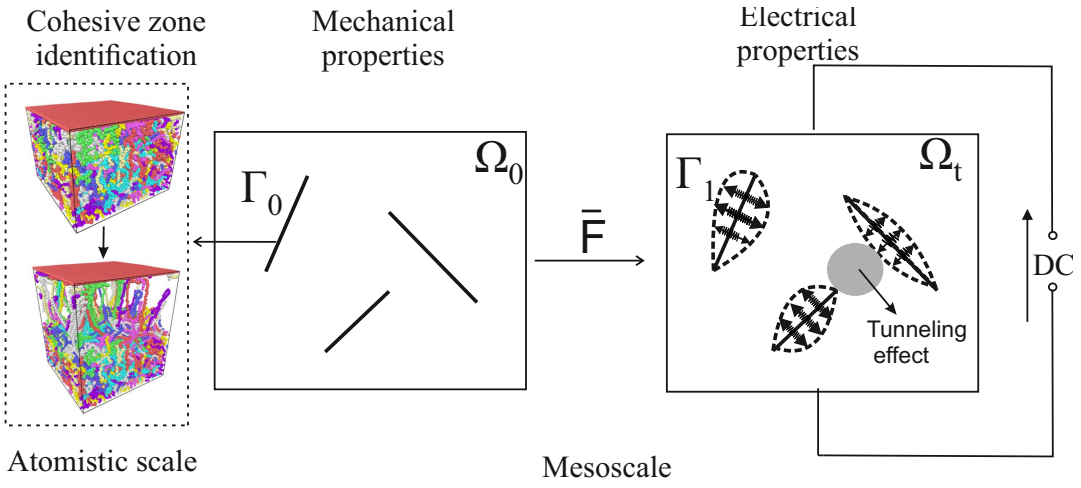

FIGURE 1 – Strategy of the multiscale modeling for study the electromechanical coupling of graphene/polymer nanocomposites.

potential [6] is employed in the simulation. For simplicity, we assume that the system is nonpolar, *i.e.* the electrostatic term in the nonbonded part of potential energy are neglected.

The initial system is prepared from the self-avoiding random walk combining the molecular dynamics relaxation steps [1].

To study the separation in opening mode, graphene was moved in successive steps of 0.5 along the Z direction following by a minimization procedure. The graphene atoms and bottom layer of the polymer were kept fixed (see Fig. 2(a)). The separation process is depicted in Figs. 2. The polymer chains undergo stretch at the beginning along the Z direction, then form highly oriented structures, called fibrils or nanofibrils. Voids appear between the fibrils during the decohesion. This deformation mechanism observed during the simulation is similar to the nano-crazes of some semi-crystalline polymers, such as polybutene [7, 8]. The size of the void grows along the separation direction ; and the extended chains slide along the graphene sheet to increase the fibrils as described in [9]. It should be noted that the separation is controlled by the chain desorption at the graphene surface by sliding, which is dominated by van der Walls interaction.

The average force of polymer on graphene was monitored, as from which we can get the normal traction force, t_n of cohesive zone as a function of the displacement of graphene layer, $[\![u_n]\!]$, as shown in Fig. 3. The force varies linearly with the displacement of graphene sheet at the which corresponds to the domain where the behavior of the interface is reversible. Then the curve bends to reach a maximum at 0.7nm, called the yield threshold. This phase corresponds to the nano-fribils creation and to the cavity initiation. Once the yield threshold crosses, the force decreases with the displacement of graphene sheet. During this phase, the chains slip on the graphene sheet to feed the fibrils. It is likely that the observed softening is related to the reduction of the contact area between polymer chains and graphene. The MD results are fitted with the following empirical model :

$$t_n = g_{cz}\left([\![u_n]\!]\right) = \begin{cases} -1529[\![u_n]\!]^2 + 2150[\![u_n]\!] & \text{if } 0 \leq [\![u_n]\!] < 0.7 \\ \frac{65}{[\![u_n]\!]^8} - \frac{4.31}{[\![u_n]\!]^{14}} + 263.74 & \text{if } 0.7 \leq [\![u_n]\!] \leq 1.15 \\ 360\exp(-0.16[\![u_n]\!]) - 15.12 & \text{if } [\![u_n]\!] > 1.15 \end{cases} \quad (1)$$

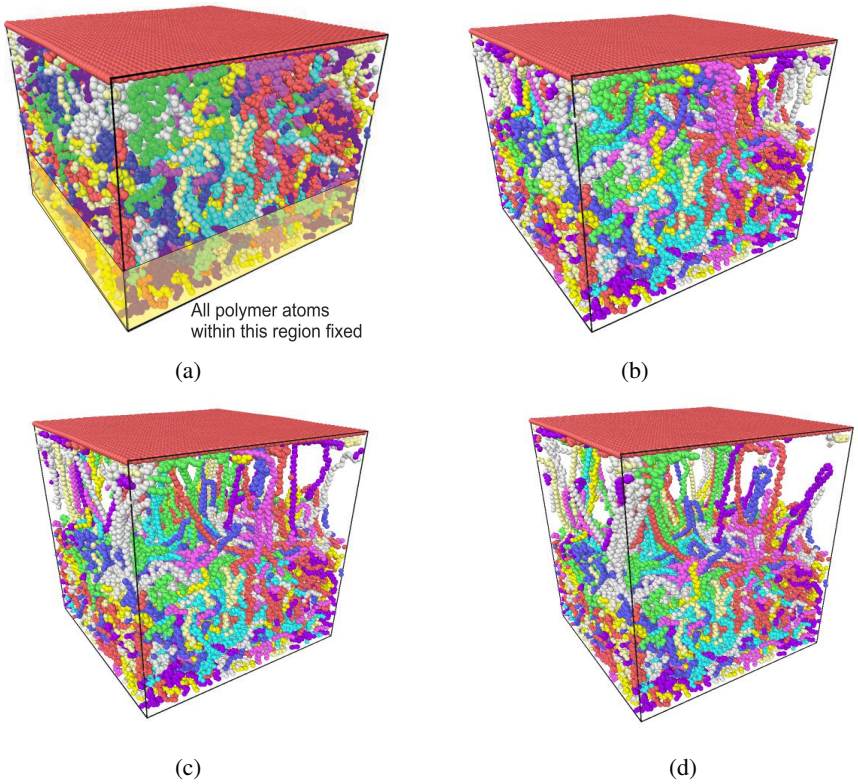

FIGURE 2 – Evolution of the atomistic model during the normal separation. The model contains 44860 atoms, and the graphene is moved with a step of 0.5 . The graphene atoms and the bottom layer of the polymer are fixed during the relaxation.

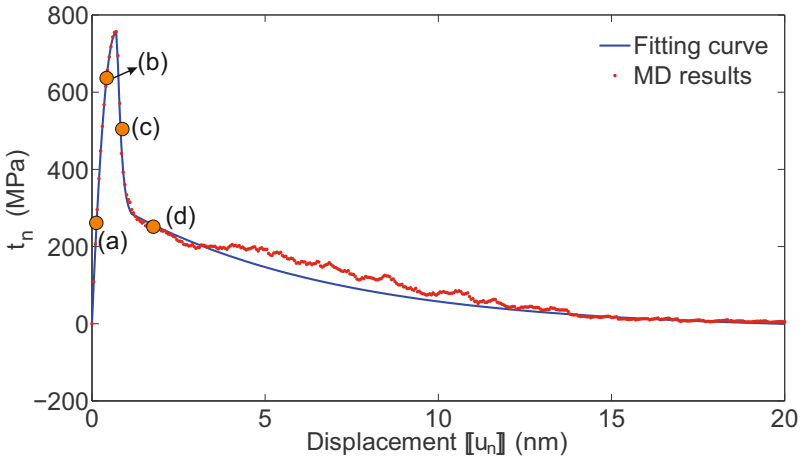

FIGURE 3 – Traction force, t_n vs displacement of graphen layer $[\![u_n]\!]$. The points denote the MD results and the line is the fitting curve. There is a correspondence between the bold points with the letters (a-d) on the curve and the Figs. 2(a-d).

3 Mechanical modeling

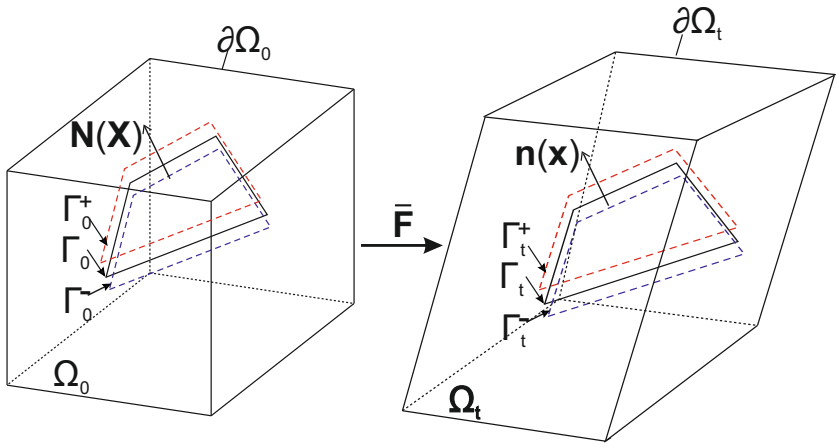

FIGURE 4 – RVE model of the graphene-reinforced nanocomposite.

Consider a continuum body Ω in the reference configuration $\Omega_0 \in \mathbb{R}^3$, and the spatial configuration $\Omega_t \in \mathbb{R}^3$. The boundary of Ω_0 are denoted by $\partial\Omega_0$ in reference configurance and $\partial\Omega_t$ in actual configuration. In the reference configuration, the graphene sheets are distributed randomly in the domain as the internal discontinuity $\Gamma_0^{(n)}$ $(n = 1, 2, \ldots, N)$, as shown in Fig. 4. The graphene surfaces and their boundary are collectively denoted by $\Gamma_0 = \cup_n \Gamma_0^{(n)}$ and $\partial\Gamma_0 = \cup_n \partial\Gamma_0^{(in)} \cup \partial\Gamma_0^{(out)}$ where $\partial\Gamma_0^{(in)} = \partial\Omega_0 \cap \partial\Gamma_0$. The two sides of the interface are denoted by Γ_0^+ and Γ_0^-. And the unit vector normal to the interface in the reference configuration is $\mathbf{n}(\mathbf{X})$. The displacement of the bulk, and the two sides of the interface are $\mathbf{u}$, $\mathbf{u}^-$ and $\mathbf{u}^+$ respectively. The current positions, $\mathbf{x}$ of the material particles at the inital position, $\mathbf{X}$, are defined by $\mathbf{x} = \mathbf{X} + \mathbf{u}$ for the bulk. $\mathbf{x}^-$ and $\mathbf{x}^+$ are the current position for the two sides of interface. The graphene sheets are modeled as the general imperfect interface [10, 11], satisfying $[\![\mathbf{u}]\!] = \mathbf{u}^+ - \mathbf{u}^- \neq 0$ and $[\![\mathbf{x}]\!] \neq 0$, the traction through the graphene surfaces is also discontinous, $[\![\mathbf{t}]\!] = \mathbf{t}^+ - \mathbf{t}^- \neq 0$ where $\mathbf{t}^+$ and $\mathbf{t}^-$ are respectively the traction on Γ_0^+ and Γ_0^- associated to the normal $\mathbf{n}(\mathbf{X})$.

3.1 Internal virtual work

In this section we follow the theory of imperfect interface at finite strains developed by Javili *et al* [11]. The internal virtual work, δW_{int}, is given in reference configuration by the contributions of polymer bulk and graphene sheets, which are modeled by imperfect interfaces :

$$\delta W_{int}(\mathbf{u}, \delta\mathbf{u}) = \delta W_{int}^{(b)}(\mathbf{u}, \delta\mathbf{u}) + \delta W_{int}^{(s)}(\mathbf{u}, \delta\mathbf{u}) \tag{2}$$

Using the second Piola-Kirchhoff stress tensor $\mathbf{S}$ (resp. the surface second Piola-Kirchhoff stress tensor, $\mathbf{S}^s$), we achieve finally the following expression of internal virtual work (for a configuration in static equilibrium) in the form :

$$\delta W_{int}^{(b)}(\mathbf{u}, \delta\mathbf{u}) = \int_{\Omega_0} \mathbf{S} : \delta\boldsymbol{\varepsilon}\, \mathrm{d}V \tag{3}$$

$$\delta W_{int}^{(s)}(\mathbf{u}, \delta\mathbf{u}) = \int_{\Gamma_0} \mathbf{S}^{\mathbf{s}} : \delta\boldsymbol{\varepsilon}^{\boldsymbol{s}} + \{\{\mathbf{t}\}\}.[\![\delta\mathbf{u}]\!]\, \mathrm{d}S \tag{4}$$

where $\delta\boldsymbol{\varepsilon}$ (resp. $\delta\boldsymbol{\varepsilon}^{\boldsymbol{s}}$) is the variation of the symmetric Green-Lagrange strain tensor, $\boldsymbol{\varepsilon} = \frac{1}{2}(\mathbf{F}^T\mathbf{F} - \mathbf{I})$ (resp. the variation of the surface Green-Lagrande strain tensor, $\boldsymbol{\varepsilon}^{\boldsymbol{s}} = \mathbf{I}_0^{\mathbf{s}}\boldsymbol{\varepsilon}\mathbf{I}_0^{\mathbf{s}}$). Here, $\mathbf{I}_0^{\mathbf{s}} = \mathbf{I} -$

$\mathbf{n}(\mathbf{X}) \otimes \mathbf{n}(\mathbf{X})$ is the projector into the tangente plan of interface in the reference configuration. $\{\{\mathbf{t}\}\} = 1/2\left(\mathbf{t}^{+} + \mathbf{t}^{-}\right)$ is the average of traction.

3.2 Constitutive laws

We choose the Saint Venant-Kirchhoff model for bulk part, which is an extension of the linear elastic material model, the second Piola-Kirchoff stress is given by :

$$\mathbf{S} = \mathbb{C}^{(b)} : \boldsymbol{\varepsilon} \tag{5}$$

where $\mathbb{C}^{(b)}$ is the forth order tensor of stiffness. It is assume to be isotropic and defined by Lame's coefficient $\lambda^{(b)} = 6890$ MPa and $\mu^{(b)} = 680$ MPa [3]. These elastic parameters are identified by MD simulations.

Like for the bulk, we assume for sake of simplicity that the behavior of imperfect interface is reversible. The surface elastic behavior of graphene is assumed to isotropic inside its plane, so the surface second Piola-Kirchoff stress is given also by Saint Venant-Kirchhoff model :

$$\mathbf{S^s} = 2\mu^{(s)}\boldsymbol{\varepsilon^s} + \lambda^{(s)}\left(\boldsymbol{\varepsilon^s} : \mathbf{I_0^s}\right)\mathbf{I_0^s} \tag{6}$$

where the surface Lame's coefficient $\lambda^{(s)} = 19.0$ N.m^{-1} and $\mu^{(s)} = 18.7$ N.m^{-1} are identified by MD simulations [3].

The expression of traction $\{\{\mathbf{t}\}\}$ is assume to be aligned with the displacement jump $[\![\mathbf{u}]\!]$ and given by :

$$\{\{\mathbf{t}\}\} = g_{cz}\left([\![\mathbf{u}]\!]\right)\frac{[\![\mathbf{u}]\!]}{||[\![\mathbf{u}]\!]||} \tag{7}$$

where $g_{cz}\left([\![\mathbf{u}]\!]\right)$ is the function identified by MD simulations in Eq. 1.

4 Electro-mechanical coupling examples

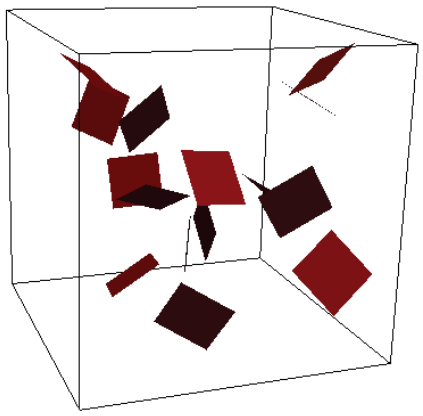

FIGURE 5 – RVE for the graphene/polymer nanocomposites involving 15 graphene square sheets in a cube of 70×70×70 nm^3.

We use this FEM framework to investigate the effective properties of graphene reinforced nanocomposites with various graphene volume fraction in linear regime. The volume fraction is controled by increasing the number of graphene sheets in the domain. The generation of the random RVEs is provided in [1]. The in-plane dimensions of graphene sheets are $15 \times 15\ nm^2$ and the RVE side length of the

cubic domain is 70 nm. We consider multi-layer graphene platelets, also called here sheets, which have a finite thickness, $h = 0.2$ nm. In this study, the graphene sheet are modeled by square plane with the side length $L = 15$ nm. One example of isotropic graphene nanocomposite RVE is illustrated in Fig. 5.

4.1 Electrical model of graphene-reinforced composites

A numerical model for electric properties of graphene/polymer nanocomposites has been proposed in [2]. In this section, we use the deformed RVE in actual conficuration Ω_t providing from mechanical simulations. The graphene sheets are assumed to be in the middle of imperfect interface Γ_t. Electric tunneling effect between graphene sheets originating from the nanoscale is taken into account.

The electric power, $\mathcal{P}_{elec}$ of the system in actual configuration is defined by

$$\mathcal{P}_{elec} = \int_{\Omega_t} \omega^{(b)}(\mathbf{x})\,\mathrm{d}V + \int_{\Gamma_t} \omega^{(s)}(\mathbf{x})\,\mathrm{d}S, \tag{8}$$

where the density functions $\omega^{(b)}$ and $\omega^{(s)}$ are the bulk and surface density functions expressed by

$$\omega^{(b)}(\mathbf{x}) = \frac{1}{2}\mathbf{j}(\mathbf{x}).\mathbf{E}(\mathbf{x}), \text{ and } \quad \omega^{(s)}(\mathbf{x}) = \frac{1}{2}\mathbf{j}^{\mathbf{s}}(\mathbf{x}).\mathbf{E}^{\mathbf{s}}(\mathbf{x}). \tag{9}$$

In these equations above, $\mathbf{E}(\mathbf{x})$ and $\mathbf{j}(\mathbf{x})$ denote to the electric field and current density respectively, and $\mathbf{E}(\mathbf{x})$ is related to the electric potential ϕ by $\mathbf{E}(\mathbf{x}) = -\nabla_x\phi(\mathbf{x})$ where ∇_x is the gradient with respect to the Eulerian coordinate, $\mathbf{x}$. Besides, $\mathbf{E}^{\mathbf{s}}(\mathbf{x})$ and $\mathbf{j}^{\mathbf{s}}(\mathbf{x})$ are the surface electric field and surface current density with respect to the graphene sheets, where $\mathbf{E}^{\mathbf{s}} = \mathbf{I}^{\mathbf{s}}_{\mathbf{t}}.\mathbf{E}$ with $\mathbf{I}^{\mathbf{s}}_{\mathbf{t}} = \mathbf{I} - \mathbf{n}(\mathbf{x}) \otimes \mathbf{n}(\mathbf{x})$ the projector operator characterizing the projection of a vector along the tangent plane to Γ_t at a point $\mathbf{x} \in \Gamma_t$ and $\mathbf{n}(\mathbf{x})$ is the unit normal vector to Γ_t in actual configuration.

The local constitutive equations relating $\mathbf{j}$ and $\mathbf{E}$ are nonlinear as :

$$\mathbf{j} = \begin{cases} \mathbf{K}^{(\mathbf{p})}_{\mathbf{0}}\mathbf{E} & \text{if } d(\mathbf{x}) > d_{cut}, \\ \mathcal{G}(\mathbf{E}, d(\mathbf{x}))\frac{\mathbf{E}}{|\mathbf{E}|} & \text{if } d(\mathbf{x}) < d_{cut} \end{cases} \tag{10}$$

where d_{cut} is a cut-off distance above which the tunneling effect can be neglected, and $\mathbf{K}^{(\mathbf{p})}_{\mathbf{0}}$ is the second-order tensor of electric conductivity of the polymer when neglecting tunneling effect. The polymer matrix is assumed to have an isotropic conductivity, *i.e.* $\mathbf{K}^{(\mathbf{p})}_{\mathbf{0}} = k^{(p)}_0\mathbf{I}$. Note that the relatively high value of $k^{(p)}_0 = 10^{-10}$ S.m^{-1} for polymer is choosen to assure the convergence of FEM framework to due the very high contrast between the conductivity of graphene and polymer matrix. The field, $d(\mathbf{x})$, called the distance function, is defined as the sum of the two smallest distances between the position $\mathbf{x}$ and the two neighbouring graphene sheets. This function is updated for all deformed configurations of RVE.

An explicit formula for the electric tunneling effect through a potential square barrier was first derived by Simmons [12] as :

$$\mathcal{G}\left(\mathbf{E}, d\left(\mathbf{x}\right)\right) = \frac{2.2e^3}{8\pi h_p \Phi_0}\left\|\mathbf{E}\right\|^2 \exp\left[-\frac{8\pi\Phi_0\sqrt{2m\Phi_0}}{2.96h_p e}\frac{1}{\left\|\mathbf{E}\right\|}\right]\ldots \tag{11}$$

$$+\frac{3e^2\sqrt{2m\Phi_0}}{2h_p^2}\left\|\mathbf{E}\right\|\exp\left[-\frac{4\pi\sqrt{2m\Phi_0}}{h_p}\frac{1}{d(\mathbf{x})}\right] \tag{12}$$

where Φ_0 is the energy barrier height that the electrons cross and h_p, e and m denote Plank's constant, the charge of an electron and a material parameter.

The surface current density $\mathbf{j}^{\mathbf{s}}$ of the graphene sheet Γ_t is related to the surface electric field, $\mathbf{E}^{\mathbf{s}}$ through :

$$\mathbf{j}^{\mathbf{s}}(\mathbf{x}) = \mathbf{K}^{(\mathbf{s})}\mathbf{E}^{\mathbf{s}} \tag{13}$$

where

$$\mathbf{K}^{(\mathbf{s})} = h\mathbf{K}^{\star}, \quad \mathbf{K}^{\star} = \mathbf{K}^{(\mathbf{g})} - \frac{\left(\mathbf{K}^{(\mathbf{g})}\mathbf{n}(\mathbf{x})\right) \otimes \left(\mathbf{K}^{(\mathbf{g})}\mathbf{n}(\mathbf{x})\right)}{\mathbf{K}^{(\mathbf{g})} : (\mathbf{n}(\mathbf{x}) \otimes \mathbf{n}(\mathbf{x}))}. \tag{14}$$

Here, h is the thickness of graphene sheets and $\mathbf{K}^{(\mathbf{g})}$ denotes the second-order electric conductivity tensor of the bulk graphite, which is given by

$$\mathbf{K}^{(\mathbf{g})} = k_{\parallel}^{(g)}\mathbf{I}_{\mathbf{t}}^{(\mathbf{s})} + k_{\perp}^{(g)}\mathbf{n}(\mathbf{x}) \otimes \mathbf{n}(\mathbf{x}) \tag{15}$$

where $k_{\parallel}^{(g)} = 83200$ S.m^{-1} and $k_{\perp}^{(g)} = 83.2$ S.m^{-1} are the conductivity parameter of graphen multilayer from [13].

We use a FEM to discretize the solution space, linear tetrahedrons for bulk part and linear triangles for graphene sheets. A Newton-Raphson procedure is used to solve this non-linear problem step by step at small increment, $\Delta\overline{\mathbf{E}}$, of effective electric field [2].

The problem being nonlinear, the effective conductivity is the incremental one dependent on the intensity and history of the applied electric field, which is defined as

$$\left(\overline{K}_T\right)_{ij}(\bar{\mathbf{E}}) = \frac{\partial \bar{j}_i(\bar{\mathbf{E}})}{\partial \bar{E}_j} \tag{16}$$

where $\bar{\mathbf{j}}$ and $\overline{\mathbf{E}}$ denote the effective current density and effective electric field of the RVE respectively defined by :

$$\bar{\mathbf{j}} = \frac{1}{\|\Omega_t\|}\int_{\Omega_t} \mathbf{j}\,\mathrm{d}V + \frac{1}{\|\Omega_t\|}\int_{\Gamma_t} \mathbf{j}^{(\mathbf{s})}\,\mathrm{d}S, \quad \bar{\mathbf{E}} = \frac{1}{\|\Omega_t\|}\int_{\Omega_t} \mathbf{E}\,\mathrm{d}V. \tag{17}$$

4.2 Evolution of electrical properties under stretching of the composite

In this section, we study the impact of both streching and decohesion at the graphene polymer interface on the electric conductivity. Indeed, the conductivity is controled by tunneling effect, that depends strongly of ditance between graphene. Thefore, we impose an macroscopic elongation, $\overline{\boldsymbol{\varepsilon}} = \bar{\varepsilon}_{11}\mathbf{e}_1 \otimes \mathbf{e}_1$, on the RVEs, from $\bar{\varepsilon}_{11} = 0\%$ to 10%. Due to the long comptutational time, only one RVE microstructure is randomly studied for each graphene volume fraction.

The deformed microstructures are stored for each 1% increment of deformation and the distance function, $d(\mathbf{x})$, is updated. Introducing the new distance function, the electrical conductivities at different effective strain $\bar{\varepsilon}_{11}$ are shown in Fig. 6. The boundary between insulator and condutor is defined to be 10^{-8} S/m, below which the material is supposed to be insulator. On the contrary, it is conductor. Focusing on the electrical conductivity along the direction of deformation $(\overline{K}_T)_{11}$, we can observe in Fig. 6 (a) that the mechanical deformation has little effect on the electrical conductivity of the nanocomposites when the graphene volume fraction is below the percolation threshold, $f < f_c = 0.52$ vol$\%$. When the graphene volume fraction is above the percolation threshold ($f > f_c = 0.52$ vol$\%$), the electrical conductivity $(\overline{K}_T)_{11}$ decreases with the applied elongation, but it should be noted that the

nanocomposites remains conductor. However, if the graphene volume fraction is around the percolation threshold ($f \approx f_c = 0.52$ vol%), a sharp decrease of the electrical conductivity can be seen when the nanocomposites is subjected to strain, which is regarded as a transition point from conductor to insulator. For instance, with 0.66 vol% graphene the transition point of the sample is $\overline{\varepsilon}_{11} \approx 3\%$, and with $f = f_c = 0.52$ vol% graphene it is $\overline{\varepsilon}_{11} \approx 10\%$.

Observed this typical conductor-to-insulator transition for the composite with $f = 0.66$ vol% graphene by the proposed model, we compare the effective conductivity with the results which are estimated without considering the the decohesion between graphene and polymer matrix (*i.e.* we impose $[\![\mathbf{u}]\!] = 0$). It can be seen on Fig. 6 (b) that neglecting the cohesive interface, the transition point increases from $\overline{\varepsilon}_{11} \approx 3\%$ to 8%, which shows the important role of decohesion at the interface in predicting the piezoresisitivity properties of polymer graphene nanocomposite. It is interesting to note that it is theoretically possible to design a composite which can go from conductor to insulator by varying the applied strain on the system. This transition can be induced mainly by the decohesion for weak interfaces, or only by strain for a stronger interface but for a more important applied elongation.

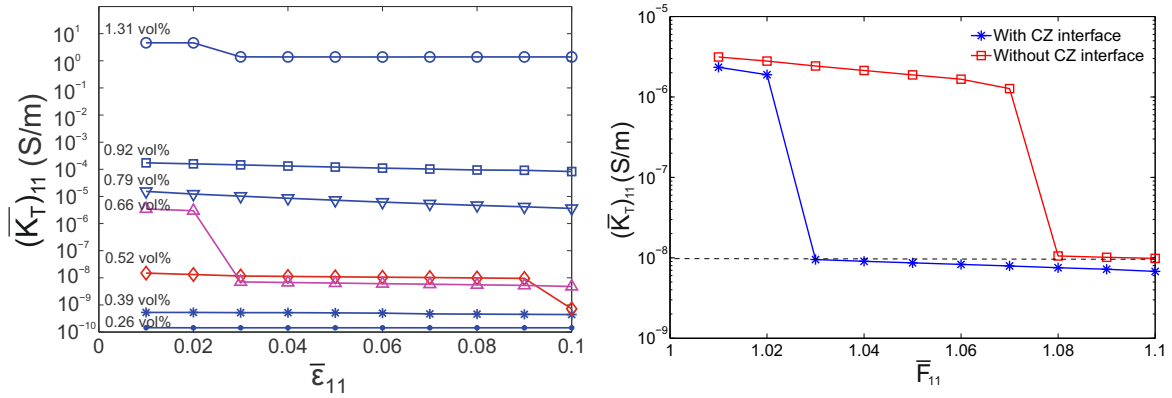

(a) (b)

FIGURE 6 – (a)Effective electrical conductivity of graphene reinforced nanocomposites, $(\overline{K_T})_{11}$, as a function of the deformation for various graphene volume fraction. Barrier height between graphene and polymer matrix is set to be 0.17 eV, and graphene aspect ratio is 75. The applied electric field is 0.0025V/nm.; (b) Effective electric conductivity $(\overline{K_T})_{11}$ as a function of effective strain $\overline{\epsilon}_{11}$ for the composite with 0.66 vol% graphene both with and without considering the cohesive interface. $\Phi_0 = 0.17$.

Moreover, the influence of barrier height, Φ_0, between graphene and polymer is presented in Fig. 7 for the configuration with 0.66 vol% graphene sheets, which is just above the percolation threshold, f_c, and exhibits the conductor-to-insulator transition. It can be noted that effective conductivity of the composites decreases with the increasing barrier height, because the tunneling current goes down along the growing barrier height according to Eq. 12 and results in [4]. For the elongation $\overline{\varepsilon}_{11} = 3\%$, the sharp decrease of the electric conductivity can be observed at both $\Phi_0 = 0.17$ eV and $\Phi_0 = 0.3$ eV. However, when the barrier height increases to 0.5 eV, the electric conductivity of the insulating composite doesn't vary a lot with the increasing effective strain. This phenomenon gives a view that the polymer matrix would also be taken into account for the material design to obtain the special electro-mehanical function.

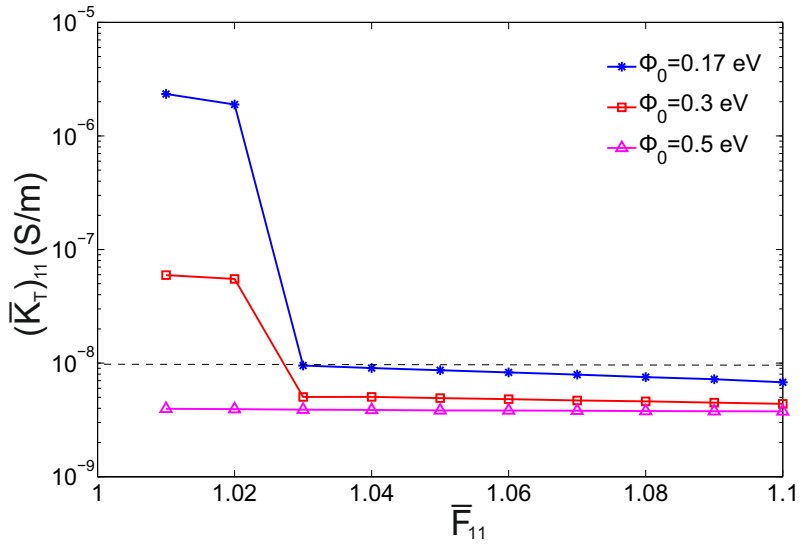

FIGURE 7 – Effective electric conductivity $(\overline{K_T})_{11}$ as a function of effective strain $\bar{\epsilon}_{11}$ for the composite with 0.66 vol$\%$ graphene at barrier height $\Phi_0 = 0.17$, 0.3 and 0.5 eV respectively.

5 Conclusion

In this paper, we identified a CZ model using MD simulations. The CZ model has enriched a nonlinear mechanical model where graphene sheets are modeled by imperfect interfaces, *i.e.* a combination of an elastic membrane and a CZ model. Finally, the mechanical model allowed us to generate deformed RVEs to study influence of strain and interfacial decohesion on the conductivity of graphene/polymer nanocomposites. An electric continuum model, that incorporates the tunneling effect, have been used to study the effective conductivity and the influence of the macroscopic elongation, the interfacial decohesion and the potential barrier height.

This multiscale and multiphysics approach has shown the existence of a piezoresistive effect for graphene/polymer nanocomposites. This effect is very significant for graphene volume fraction just above the percolation threshold because a conductor-insulator transition is observed for elongations above 2%. In addition, the model has demonstrated the importance of decohesion on the conductor-insulator transition. Indeed, the transition appears for an elongation of 8% instead of 2%, when the interfacial decohesion is removed in the mechanical model.

6 Aknowledgements

X. Lu thanks the financial support of China Scholarship Council(CSC) for the Ph.D. thesis. The molecular simulations was carried out using the LAMMPS molecular dynamics software [14]. The GMSH mesh generator are used to create all meshes [15].

Références

[1] X. Lu, F. Detrez, J. Yvonnet, J. Bai, Multiscale study of influence of interfacial decohesion on piezoresistivity of graphene/polymer nanocomposites, Modell. Simul. Mater. Sci. Eng., 27 (2018).

[2] X. Lu, J. Yvonnet, F. Detrez, J. Bai, Multiscale modeling of nonlinear electric conductivity in graphene-reinforced nanocomposites taking into account tunnelling effect, J. Comput. Phys., 337 (2017) 116-131.

[3] X. Lu, Multiscale electro-mechanical modeling of graphene/polymer nanocomposites, Thèse, Université Paris-Saclay, 2017.

[4] X. Lu, J. Yvonnet, F. Detrez, J. Bai, Low electrical percolation thresholds and nonlinear effects in graphene-reinforced nanocomposites : A numerical analysis, J. Compos. Mater., 52 (2018) 2767-2775.

[5] X .Lu, D. G. Giovanis, J. Yvonnet, V. Papadopoulos, F. Detrez, J. Bai, A data-driven computational homogenization method based on neural networks for the nonlinear anisotropic electrical response of graphene/polymer nanocomposites, Comput. Mech., (2018).

[6] S. L. Mayo, B. D. Olafson, W. A. Goddard, DREIDING : a generic force field for molecular simulations, J. Phys. Chem., 94 (1990) 8897-8909.

[7] C. Thomas, R. Seguela, F. Detrez, V. Miri, C. Vanmansart, Plastic deformation of spherulitic semicrystalline polymers : An in situ AFM study of polybutene under tensile drawing, Polymer, 50 (2009) 3714-3723.

[8] F. Detrez, Nanomécanismes de déformation des polymères semi-cristallins : étude in situ par microscopie à force atomique et modélisation, Thèse, Université Lille I, 2008.

[9] E. J. Kramer, L. L. Berger, Fundamental processes of craze growth and fracture, In : Crazing in Polymers Vol. 2, Springer, (1990) 1-68.

[10] G. Chatzigeorgiou, F. Meraghni, A. Javili, Generalized interfacial energy and size effects in composites, J. Mech. Phys. Solids, 106 (2017) 257-282.

[11] A. Javili, P. Steinmann, J. Mosler, Micro-to-macro transition accounting for general imperfect interfaces, Comput. Methods Appl. Mech. Engrg., 317 (2017) 274-317.

[12] J. G. Simmons, Electric Tunnel Effect between Dissimilar Electrodes Separated by a Thin Insulating Film, J. Appl. Phys., 34 (1963) 2581-2590.

[13] S. Stankovich, D. A. Dikin, G. H. B. Dommett, K. M. Kohlhaas, E. J. Zimney, E. A. Stach, R. D. Piner, S. T. Nguyen, R. S. Ruoff, Graphene-based composite materials, Nature, 442 (2006) 282-286.

[14] S. Plimpton, Fast parallel algorithms for short-range molecular dynamics, J. Comput. Phys., 117 (1995) 1-19.

[15] C. Geuzaine, J. F. Remacle, Gmsh : A 3-D finite element mesh generator with built-in pre- and post-processing facilities, Int. J. Numer. Methods Eng., 79 (2009) 1309-1331.